

End-On Azido-Bridged 3d–4f Complexes Showing Single-Molecule-Magnet Property

Xing-Cai Huang,[†] Chun Zhou,[†] Hai-Yan Wei,^{*,‡} and Xin-Yi Wang^{*,†}[†]State Key Laboratory of Coordination Chemistry, School of Chemistry and Chemical Engineering, Nanjing University, Nanjing 210093, China[‡]Jiangsu Key Laboratory of Biofunctional Materials, School of Chemistry and Materials Science, Nanjing Normal University, Nanjing 210097, China

Supporting Information

ABSTRACT: Four tetranuclear 3d–4f complexes with the 4f centers bridged solely by end-on azide bridges were reported. The [CuTb]₂ compound displays single-molecule-magnet behavior with hysteresis loops observed at up to 2.4 K.

Structurally characterized azido-bridged lanthanides remain relatively scarce^{1,2} despite the success of both the azide and lanthanides in the molecular magnetism.^{3,4} The underlying cause is the principle of hard and soft acids and bases (HSAB), according to which the lanthanide cations with high positive charge and low polarizability are hard Lewis acids, while the azide falls into the borderline category.⁵ Recently, the lanthanide-containing single-molecule magnets (Ln-SMMs) have invoked intense interest because of their large and/or high anisotropic magnetic moments.⁶ In the majority of the Ln-SMMs, the bridges between the lanthanides are usually oxygen atoms, with some notable exceptions in the organolanthanides where the bridges could be nitrogen, sulfur, or hydrogen.⁷ Although there exist several examples of Ln-SMMs with azide bridges (Table S1 in the Supporting Information, SI),² the lanthanides in these SMMs were usually bridged by mixed ligands of azide and some other bridges.

Given the aforementioned consideration, we tackled the chemistry of the azido-bridged lanthanides. Despite the weakness of the lanthanide–azide interaction, lanthanide azides are much easier to achieve in nonaqueous media because of the decreased competition with hydration. The widely studied heterometallic 3d–4f complexes [M²⁺LLn³⁺] (M²⁺, 3d ions; Ln³⁺, 4f ions) with compartmental Schiff-base ligands were chosen as synthetic tectons for this purpose because they are stable in solution and many of them, and their follow-up compounds, are actually SMMs.^{8–14} By carefully tuning the synthetic conditions, we successfully prepared a series of azido-bridged 3d–4f tetranuclear complexes {[MLLn](μ-N₃)_n[LnLM]} (Figure 1a) with the 3d centers ranging from the anisotropic Co²⁺, to the isotropic Cu²⁺, and to the diamagnetic Zn²⁺ centers. The 4f centers are bridged solely by the double or triple end-on (EO) azides. Here, we report the structure and SMM property of the [CuTb]₂ complex [Cu₂(valpn)₂Tb₂(N₃)₆]·2CH₃OH [**1**]_{CuTb}; H₂valpn = 1,3-propanediylbis(2-iminomethylene-6-methoxyphenol)]. Hysteresis loops were observed for **1** at up to 2.4 K, which is the

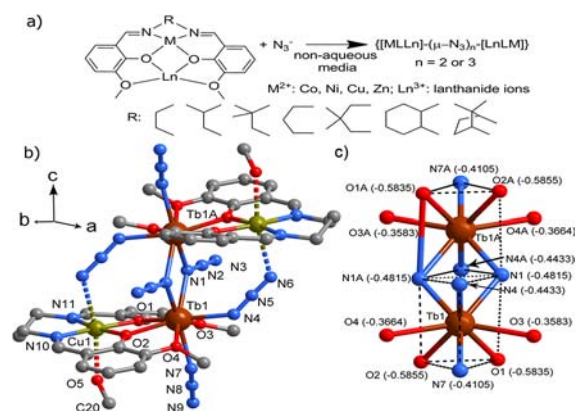


Figure 1. (a) Synthesis of the azido-bridged lanthanides {[MLLn](μ-N₃)_n[LnLM]}. (b) Structure of **1** showing the double EO azido-bridged [CuTb]₂ cluster. (c) Bicapped trigonal-prismatic environment of the Tb³⁺ ions, with the Mulliken charges of the coordinated atoms obtained from density functional theory calculations.

highest for all of the reported Cu–Ln-based SMMs. For comparison, isostructural compounds [ZnTb]₂ (**2**_{ZnTb}), [CuGd]₂ (**3**_{CuGd}), and [ZnGd]₂ (**4**_{ZnGd}) were also investigated.

1–4 were prepared by the reaction of N₃⁻ and [M(valpn)-Ln]³⁺ in a mixed solvent of methanol and acetonitrile. Lanthanide chlorides, instead of the nitrates, were used to avoid oxygen-based hard acids. All four compounds are isostructural and crystallize in the triclinic space group P $\bar{1}$ (Tables S2 and S3 in the SI). As plotted in Figure 1b for **1**, two [CuTb] units are bridged by the double EO N₃⁻ between two Tb atoms to form the [CuTb]₂ cluster. The Cu²⁺ and Tb³⁺ ions are in the N₂O₂ and O₄ pockets of valpn, respectively. The coordination geometry of Cu²⁺ can be viewed as an elongated octahedron [Cu1–O5 = 2.478(4) Å; Cu1–N6 = 2.678(4) Å], and the eight-coordinated Tb³⁺ center adopts a N₄O₄ bicapped trigonal-prismatic geometry (Figure 1c). The bond lengths for the trigonal prism are in the range of 2.341(2)–2.454(2) Å, while those for the two capping atoms are considerably large [Tb1–O3 = 2.533(2) Å; Tb1–O4 = 2.546(2) Å]. The Cu–O–Tb bond angle [Cu1–O1–Tb1 = 107.86(9)°; Cu1–O2–Tb2 = 107.75(9)°] and the dihedral angle between the Cu–O1–O2 and Tb1–O1–O2 planes [11.4 (1)°] are in the normal range

Received: April 21, 2013

Published: June 7, 2013

of the various [CuTb] compartmental compounds.^{10–13} These tetranuclear clusters are well separated from each other, with the shortest intercluster Cu...Cu, Cu...Tb, and Tb...Tb distances being 7.910, 8.153, and 10.122 Å, respectively.

Variable-temperature direct-current (dc) magnetic susceptibilities of 1–4 were measured on powder samples embedded in eicosane (Figure 2). The $\chi_M T$ values at 300 K for 1–4 are

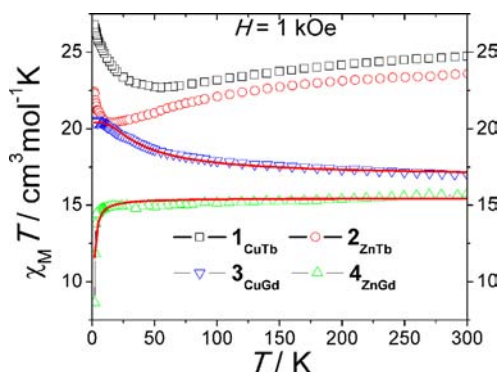


Figure 2. Temperature dependence of $\chi_M T(T)$ for compounds 1–4. The lines are fitted curves using a simple dinuclear model.

24.73, 23.60, 17.02, and 15.74 $\text{cm}^3 \text{mol}^{-1} \text{K}$, respectively, close to the calculated 24.39, 23.64, 16.51, and 15.76 $\text{cm}^3 \text{mol}^{-1} \text{K}$ (for Cu, $S = 1/2$, $g = 2$; for Gd, $S = 7/2$, $g = 2$; for Tb, $J = 6$, $g = 3/2$). For 4, the $\chi_M T$ curve remains constant down to 4 K and decreases abruptly upon further cooling, suggesting a very weak antiferromagnetic interaction between the Gd³⁺ centers. The analysis according to a dinuclear model ($H = -2J_{\text{Gd1}}S_{\text{Gd2}}$) leads to $J = -0.03 \text{ cm}^{-1}$ and $g = 1.98$ ($R = \sum[(\chi T)_{\text{obsd}} - (\chi T)_{\text{calcd}}]^2 / \sum[(\chi T)_{\text{obsd}}]^2 = 6 \times 10^{-4}$). For 3, the increase of $\chi_M T$ upon cooling indicates ferromagnetic coupling. The fitting of the data according to a linear tetranuclear model ($H = -2J_{\text{CuGd}}(S_{\text{Gd1}}S_{\text{Gd1}} + S_{\text{Gd2}}S_{\text{Gd2}}) - 2J_{\text{GdGd}}S_{\text{Gd1}}S_{\text{Gd2}}$) leads to $J_{\text{CuGd}} = 4.18 \text{ cm}^{-1}$, $J_{\text{GdGd}} = -0.001 \text{ cm}^{-1}$, and $g = 2.02$ ($R = 3 \times 10^{-5}$). As the temperature is lowered, the $\chi_M T$ values of 1 and 2 first decrease to 22.69 and 15.99 $\text{cm}^3 \text{mol}^{-1} \text{K}$ at 55 and 16 K and then increase to 26.79 and 22.51 $\text{cm}^3 \text{mol}^{-1} \text{K}$ at 2 K, respectively. The profile of these $\chi_M T$ curves suggests depopulation of the Tb³⁺ Stark levels and ferromagnetic Tb³⁺–Tb³⁺ and Cu²⁺–Tb³⁺ interactions. The isothermal magnetization curves at 2 K for 1–4 were also measured (Figure S9 in the SI). The magnetization values at 70 kOe ($M_s = 10.6, 9.2, 16.4, \text{ and } 13.9 \mu_B$ for 1–4) are very close to the spin-only values for 3 and 4 and to the values in the literature for 1 and 2.^{9–12}

To investigate the dynamic of the magnetization, alternating-current (ac) susceptibilities under a zero dc field were measured for 1 and 2. As shown in Figures 3a and S10 in the SI, obvious frequency-dependent ac signals were observed for 1, as expected for a SMM. The χ_M'' curves show frequency-dependent peaks between 2.6 and 6.6 K in the frequency range of 1–1500 Hz. The fact that both χ_M' and χ_M'' tend to vanish at low temperatures suggests the efficient suppression of the quantum tunnelling of magnetization (QTM) often seen in lanthanide SMMs.⁶ The frequency-dependent ac data measured from 3 to 6 K were displayed as $\chi_M''(\nu)$ in Figure S11 in the SI and as Cole–Cole plots in Figure S12 in the SI. The Cole–Cole plots can be fitted well to the generalized Debye model, with α parameters below 0.12 (Table S4 in the SI), indicating a very narrow distribution of relaxation processes.¹⁵ The

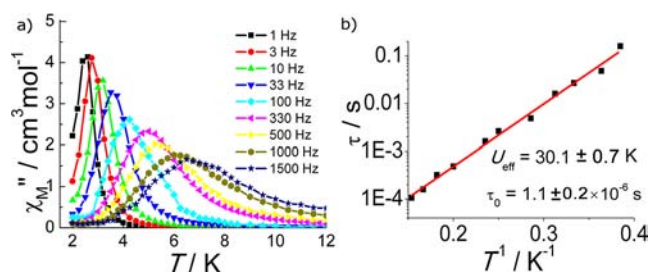


Figure 3. (a) Temperature dependence of out-of-phase ac susceptibilities for 1 under $H_{\text{ac}} = 3 \text{ Oe}$ and $H_{\text{dc}} = 0 \text{ Oe}$. (b) Arrhenius plot of 1.

magnetic relaxation time (τ) as a function of $1/T$ derived from the ac data, as plotted in Figure 3b, shows a thermally activated process and can be fitted to an Arrhenius law, $\tau = \tau_0 \exp(U_{\text{eff}}/k_B T)$, with the effective barrier $U_{\text{eff}} = 30.1 \pm 0.7 \text{ K}$ ($20.9 \pm 0.5 \text{ cm}^{-1}$) and $\tau_0 = 1.1 \pm 0.2 \times 10^{-6} \text{ s}$. For 2, frequency-dependent out-of-phase signals could also be observed under 5 K (Figure S13 in the SI), indicating the onset of slow magnetic relaxation. However, no peaks could be observed down to 2 K.

Slow magnetic relaxation (τ is estimated to be about 3.8 s from the Arrhenius law at 2 K) of 1 was further confirmed by the magnetic hysteresis loops measured on a conventional SQUID vibrating sample magnetometer. As plotted in Figure 4,

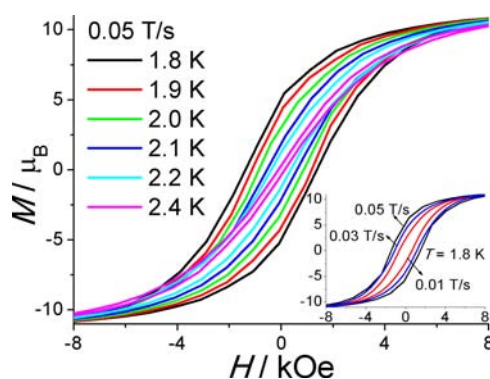


Figure 4. Hysteresis loops of 1 measured on the powder samples on a conventional SQUID vibrating sample magnetometer at the indicated temperatures and field sweep rates.

the loops can be observed up to 2.4 K at a sweep rate of 0.05 T s^{-1} . The coercive field of these loops increases with decreasing temperature and increasing field sweep rate, as expected for a SMM.

The origin of the SMM behavior of 1 is worthy of further discussion. It is now a consensus that the high global magnetic anisotropy is the most important to achieve better SMMs.^{6,16} However, magnetic anisotropy is also the most difficult to design and control, especially for the lanthanides with very complex f orbitals. Nevertheless, a qualitative method for predicting the desired ligand-field environments favoring magnetic anisotropy for the f-element ions has been proposed and tested in several cases.^{6c,12a–c,14b} It was proposed that axially coordinated ligand environments are suitable for the Dy³⁺, Tb³⁺, and Ho³⁺ ions, which have a prolate shape of the electron density, to generate easy-axis anisotropy. To estimate the negative charge distributions surrounding the Tb³⁺ ions, density functional theory calculations were performed using the

structural parameters obtained from the X-ray data of **1**. The resulting Mulliken charges are shown in Figure 1c. It is obvious that the negative charges for O3 and O4 (−0.3583 and −0.3664) are considerably less than those of the trigonal prism, resulting an obvious axial ligand-field architecture and axial anisotropy.

Easy-axis anisotropy of the Tb³⁺ centers of **1** and **2** is not sufficient to fulfill their SMM properties. To achieve the bistable ground state for the non-Kramers Tb³⁺ ion, a strict axial symmetry such as that in the double-decker [TbPc₂]ⁿ compounds¹⁷ and/or the proper magnetic coupling, as demonstrated in the radical-bridged Tb₂ compounds,¹⁸ will be required. For many of the reported CuTb-based SMMs, their blocking temperatures (T_B) are often very low, and an external dc field is often required to suppress the QTM and to observe the peaks of χ_M^{''} above 1.8 K.^{10,12c,d} Lower temperatures (typically <1 K) are usually needed to observe the hysteresis loops.^{10,12b} Considering the low symmetry of the Tb³⁺ centers in **1** and **2**, both the Cu–Tb and Tb–Tb magnetic interactions are believed to be vital. It has been demonstrated in the literature that the Cu–Tb interaction plays an essential role in achieving the SMM behavior by suppressing the rhombic component of the crystal field acting on the Tb³⁺ ions.^{9,11} The increase of the T_B value of **1** compared to the reported systems where the [CuTb] units are magnetically isolated from each other^{8–12} does suggest the great value of the Tb–Tb interaction. However, the lower T_B value of **2** suggests that the Tb–Tb interaction alone is not enough to suppress the QTM, probably because of its weakness. These results give a clear conclusion that both the 3d–4f and 4f–4f magnetic interactions are important for the SMM properties and warrant further synthetic efforts, which are currently focused on only either the 3d–4f or the 4f–4f interaction.

In conclusion, we demonstrated the structures and magnetic properties of four tetranuclear 3d–4f complexes where the lanthanides are bridged solely by the EO azides. The [CuTb]₂ compound is a SMM with an effective barrier of 30.1 K (20.9 cm^{−1}) and with hysteresis loops observed at up to 2.4 K. More results of the related compounds will be reported in due course.

■ ASSOCIATED CONTENT

■ Supporting Information

X-ray crystallographic files (CIF), experimental details, crystallographic data, and additional structural and magnetic figures. This material is available free of charge via the Internet at <http://pubs.acs.org>.

■ AUTHOR INFORMATION

Corresponding Author

*E-mail: weihaiyan@nynu.edu.cn (H.-Y.W.), wangxy66@nju.edu.cn (X.-Y.W.).

Notes

The authors declare no competing financial interest.

■ ACKNOWLEDGMENTS

This work was supported by the 973 Program (2013CB922102), NSFC (91022031, 21021062, and 21101093), and NSF of JiangSu Province (BK2011548).

■ REFERENCES

(1) (a) Walter, M. D.; Weber, F.; Wolmershäuser, G.; Sitzmann, H. *Angew. Chem., Int. Ed.* **2006**, *45*, 1903. (b) Evans, W. J.; Montalvo, E.;

Champagne, T. M.; Ziller, J. W.; Dipasquale, A. G.; Rheingold, A. L. *J. Am. Chem. Soc.* **2008**, *130*, 16. (c) Starynowicz, P.; Bukietyńska, K.; Ryba-romanowski, W.; Dominiak-dzik, G.; Gołab, St. *Polyhedron* **1994**, *13*, 1069.

(2) (a) Ako, A. M.; Mereacre, V.; Clérac, R.; Wernsdorfer, W.; Hewitt, I. J.; Anson, C. E.; Powell, A. K. *Chem. Commun.* **2009**, 544. (b) Burrow, C. E.; Burchell, T. J.; Lin, P. H.; Habib, F.; Wernsdorfer, W.; Clérac, R.; Murugesu, M. *Inorg. Chem.* **2009**, *48*, 8051. (c) Rinck, J.; Novitchi, G.; Heuvel, W. V.; Ungur, L.; Lan, Y.; Wernsdorfer, W.; Anson, C. E.; Chibotaru, L. F.; Powell, A. K. *Angew. Chem., Int. Ed.* **2010**, *49*, 7583. (d) Anwar, M. U.; Thompson, L. K.; Dawe, L. N.; Habib, F.; Murugesu, M. *Chem. Commun.* **2012**, *48*, 4576. (e) Lin, S. Y.; Zhao, L.; Guo, Y. N.; Zhang, P.; Guo, Y.; Tang, J. K. *Inorg. Chem.* **2012**, *51*, 10522. (f) Schmidt, S.; Prodius, D.; Mereacre, V.; Kostakis, G. E.; Powell, A. K. *Chem. Commun.* **2013**, *49*, 1696. (g) Guo, P. H.; Liao, X. F.; Leng, J. D.; Tong, M. L. *Acta Chim. Sin.* **2013**, *71*, 173.

(3) (a) Ribas, J.; Escuer, A.; Monfort, M.; Vicente, R.; Cortés, R.; Lezama, L.; Rojo, T. *Coord. Chem. Rev.* **1999**, *193–195*, 1027. (b) Wang, X. Y.; Wang, Z. M.; Gao, S. *Chem. Commun.* **2008**, 281.

(4) Benelli, C.; Gatteschi, D. *Chem. Rev.* **2002**, *102*, 2369.

(5) (a) Pearson, R. G. *J. Chem. Educ.* **1968**, *45*, 581. (b) Pearson, R. G. *J. Chem. Educ.* **1968**, *45*, 643.

(6) (a) Woodruff, D. N.; Winpenny, R. E. P.; Layfield, R. A. *Chem. Rev.* DOI:10.1021/cr400018q. (b) Sessoli, R.; Powell, A. K. *Coord. Chem. Rev.* **2009**, *253*, 2328. (c) Rinehart, J. D.; Long, J. R. *Chem. Sci.* **2011**, *2*, 2078–2085.

(7) (a) Tuna, F.; Smith, C. A.; Bodensteiner, M.; Ungur, L.; Chibotaru, L. F.; McInnes, E. J. L.; Winpenny, R. E. P.; Collison, D.; Layfield, R. A. *Angew. Chem., Int. Ed.* **2012**, *51*, 6976. (b) Venugopal, A.; Tuna, F.; Spaniol, T. P.; Ungur, L.; Chibotaru, L. F.; Okuda, J.; Layfield, R. A. *Chem. Commun.* **2013**, *49*, 901. (c) Layfield, R. A.; McDouall, J. J. W.; Sulway, S. A.; Tuna, F.; Collison, D.; Winpenny, R. E. P. *Chem.—Eur. J.* **2010**, *16*, 4442.

(8) Andruh, M. *Chem. Commun.* **2011**, 47, 3025.

(9) Osa, S.; Kido, T.; Matsumoto, N.; Re, N.; Pochaba, A.; Mrozinski, J. *J. Am. Chem. Soc.* **2004**, *126*, 420.

(10) (a) Costes, J. P.; Dahan, F.; Wernsdorfer, W. *Inorg. Chem.* **2006**, *45*, 5. (b) Costes, J. P.; Auchel, M.; Dahan, F.; Peyrou, V.; Shova, S.; Wernsdorfer, W. *Inorg. Chem.* **2006**, *45*, 1924. (c) Novitchi, G.; Costes, J. P.; Tuchagues, J. P.; Vendier, L.; Wernsdorfer, W. *New J. Chem.* **2008**, *32*, 197.

(11) Klokishner, S. I.; Ostrovsky, S. M.; Reu, O. S.; Pali, A. V.; Tregenna-Piggott, P. L. W.; Brock-Nannestad, T.; Bendix, J.; Mutka, H. *J. Phys. Chem. C* **2009**, *113*, 8573.

(12) (a) Kajiwara, T.; Nakano, M.; Takaishi, S.; Yamashita, M. *Inorg. Chem.* **2008**, *47*, 8604. (b) Kajiwara, T.; Takahashi, K.; Hiraizumi, T.; Takaishi, S.; Yamashita, M. *CrystEngComm* **2009**, *11*, 2110. (c) Kajiwara, T.; Nakano, M.; Takahashi, K.; Takaishi, S.; Yamashita, M. *Chem.—Eur. J.* **2011**, *17*, 196. (d) Shiga, T.; Miyasaka, H.; Yamashita, M.; Morimoto, M.; Irie, M. *Dalton Trans.* **2011**, *40*, 2275.

(13) Feng, X. J.; Zhou, W. Z.; Li, Y. G.; Ke, H. S.; Tang, J. K.; Clérac, R.; Wang, Y. H.; Su, Z. M.; Wang, E. B. *Inorg. Chem.* **2012**, *51*, 2722.

(14) (a) Novitchi, G.; Wernsdorfer, W.; Chibotaru, L. F.; Costes, J. P.; Anson, C. E.; Powell, A. K. *Angew. Chem., Int. Ed.* **2009**, *48*, 1614. (b) Yamashita, A.; Watanabe, A.; Akine, S.; Nabeshima, T.; Nakano, M.; Yamamura, T.; Kajiwara, T. *Angew. Chem., Int. Ed.* **2011**, *50*, 4016.

(15) Cole, K. S.; Cole, R. H. *J. Chem. Phys.* **1941**, *9*, 341.

(16) (a) Waldmann, O. *Inorg. Chem.* **2007**, *46*, 10035. (b) Neese, F.; Pantazis, D. A. *Faraday Discuss.* **2011**, *148*, 229.

(17) Ishikawa, N.; Sugita, M.; Ishikawa, T.; Koshihara, S.; Kaizu, Y. *J. Am. Chem. Soc.* **2003**, *125*, 8694.

(18) Rinehart, J. D.; Fang, M.; Evans, W. J.; Long, J. R. *J. Am. Chem. Soc.* **2011**, *133*, 14236.